(11) C. K. Chou, D. L. Miles, R. Bau, and T. C. Flood, *J. Am. Chem. Soc.*, preceding paper in this issue.
(12) The absorption correction used is based on the variation in intensity of an axial reflection (at $\chi = 90°$) with spindle angle $\Phi$; see T. D. Furnas, "Single-Crystal Orienter Manual", General Electric Co., Milwaukee, Wis., 1966.
(13) The major computations in this work were performed on the USC IBM 370-155 computer using CRYM, an amalgamated set of crystallographic programs developed by Dr. Richard Marsh's group at the California Institute of Technology.
(14) $R = \Sigma||F_o| - |F_c||/\Sigma|F_o|$; $R_w = [\Sigma w(|F_o| - |F_c|)^2/\Sigma wF_o^2]^{1/2}$.
(15) W. C. Hamilton, *Acta Crystallogr.*, **18**, 502 (1965).
(16) G. Kartha, F. R. Ahmed, and W. H. Barnes, *Acta Crystallogr.*, **15**, 326 (1962).
(17) See paragraph at end of paper regarding supplementary material.
(18) Absolute configurations of four iron complexes where chirality is at the metal have been determined crystallographically: $CpFe(CO)(PPh_3)CH_2O$(menthyl) and $CpFe(CO)(PPh_3)CH_2CO_2$(menthyl), ref 11; $CpFe(CO)(PPh_3)CO_2$(menthyl), M. G. Reisner, I. Bernal, H. Brunner, and M. Muschiol, *Angew. Chem., Int. Ed. Engl.*, **15**, 776 (1976); and $[CpFe(CO)(PPh_3)$=CMeNHCHMePh$]^+BF_4^-$, V. W. Day and A. Davison, personal communication.
(19) Structure determinations of racemic materials $CpFe(CO)(PPh_3)R$: R = $C_6H_5$, V. A. Semion and Yu. T. Struchkov, *J. Struct. Chem.*, **10**, 80 (1969); R = $C(O)C_6H_5$, *ibid.*, **10**, 563 (1969); R = α-thiophenyl, Y. G. Andrianov, G. N. Sergeeva, Yu. T. Struchkov, K. N. Anisimov, N. E. Kolobova, and A. S. Beschastnov, *ibid.*, **11**, 163 (1970).
(20) It should be noted that these generalizations (except for retention at carbon for CO insertion) apply only to the Fe–C bond in CpFe(CO)LR systems, and are based on a limited number of examples. Also, the decarbonylation was a *photochemical* reaction, and it resulted in a *formal* inversion of configuration, undoubtedly not a Walden inversion.
(21) It is important to point out that these CD correlations are only suggestive, and must be used with care. For a discussion of these correlations, see ref 11.
(22) T. C. Flood and D. L. Miles, *J. Organomet. Chem.*, **127**, 33 (1977).
(23) Even $SO_2$ is not an especially good dissociating solvent; for example, $Et_4N^+Br^-$ has a dissociation constant of ca. $5 \times 10^{-5}$ at 0 °C in liquid $SO_2$ (T. C. Waddington, "Non-Aqueous Solvents", Appleton-Century-Croft, New York, N.Y., 1969, p 43).
(24) For example, optically active *cis*-5-methyl-2-cyclohexenyl chloride racemizes prior to solvolysis in acetic acid, without detectable formation of the trans isomer (H. L. Goering, T. D. Nevitt, and E. F. Silversmith, *J. Am. Chem. Soc.*, **77**, 5026 (1955)), and *p*-chlorobenzhydryl *p*-nitrobenzoate undergoes solvolysis in aqueous acetone more slowly than racemization, which in turn is slower than exchange of the benzhydryl group between the two benzoate oxygens (H. L. Goering and J. F. Levy, *ibid.*, **86**, 120 (1964)). A review: D. J. Raber, J. M. Harris, and P. v. R. Schleyer in "Ions and Ion Pairs in Organic Reactions", Vol. 2, M. Szwarc, Ed., Wiley, New York, N.Y., 1974, p 247 ff.
(25) H. Brunner and W. Steger, *Bull. Soc. Chim. Belg.*, **85**, 883 (1976); H. Brunner and J. A. Aclasis, *J. Organomet. Chem.*, **104**, 347 (1976); H. Brunner, J. A. Aclasis, M. Langer, and W. Steger, *Angew. Chem., Int. Ed. Engl.*, **13**, 810 (1974).
(26) P. Hofmann, Angew. Chem., Int. Ed. Engl., **16**, 536 (1977).
(27) R. A. Sneen, *Acc. Chem. Res.*, **6**, 46 (1973).

# Studies on the Ferric Forms of Cytochrome P-450 and Chloroperoxidase by Extended X-ray Absorption Fine Structure. Characterization of the Fe–N and Fe–S Distances

**Stephen P. Cramer,[1a] John H. Dawson,[1b] Keith O. Hodgson,*[1a] and Lowell P. Hager[1c]**

*Contribution from the Department of Chemistry, Stanford University, Stanford, California 94305, the Division of Chemistry and Chemical Engineering, California Institute of Technology, Pasadena, California 91125, and the Department of Biochemistry, University of Illinois, Urbana, Illinois 61801.*
*Received February 3, 1978*

**Abstract:** Cytochrome P-450 and chloroperoxidase are Fe-heme proteins with similar spectroscopic properties, which catalyze respectively the hydroxylation and halogenation of organic substances. The nature of and distances to the nonporphyrin (axial) ligands in these proteins are clearly of importance in understanding their catalytic cycles on a molecular level. This paper reports the first use of extended X-ray absorption fine structure (EXAFS) spectroscopy to study the iron environment in the ferric resting states of these two enzymes. First, analysis methods were developed for model iron porphyrin systems. Least-squares curve fits to the EXAFS data, using empirical phase and amplitude functions, led to the determination of interatomic distances in Fe porphyrins of known structure; Fe–$N_P$ distances were determined to within ±0.007 Å and the Fe–$C_\alpha$ and Fe–X (where X = O, S, N) to better than ±0.025 Å. Second, visual comparison of the protein data with that for the models allowed classification of the chloroperoxidase as high spin (iron out of plane) and P-450-LM-2 as low spin (iron in plane). The data for both oxidized enzymes demonstrate the presence of an axial sulfur ligand. Finally, detailed curve fitting analysis of the EXAFS revealed that the chloroperoxidase distances were Fe–$N_P$ = 2.05 Å, Fe–$C_\alpha$ = 3.09 Å, and Fe–S = 2.30 Å. These are strikingly similar to the corresponding distances found in $Fe^{III}$(PPIXDME)($SC_6H_4$-*p*-$NO_2$). The distances from EXAFS analysis for P-450-LM-2 were 2.00, 3.07, and 2.19 Å for the Fe to $N_P$, $C_\alpha$, and axial S ligands, respectively. The use of EXAFS for determining accurate interatomic distances, atomic types, and coordination numbers in these types of iron-heme proteins is clearly demonstrated.

## Introduction

Cytochrome P-450 and chloroperoxidase are heme proteins with unusual catalytic and spectral properties. The P-450 enzymes,[2] which have been isolated from numerous sources including mammalian tissues, catalyze the hydroxylation of substrates, RH (see reaction 1), by dioxygen. One oxygen atom of dioxygen is incorporated into the substrate while the other is reduced to water, thus placing the P-450 enzymes in the monooxygenase or mixed-function oxidase classification of oxygen metabolizing enzymes. The two electron equivalents utilized in this process are provided physiologically by either a flavin or iron-sulfur protein reductase. Only one other heme protein[3] is normally capable of activating dioxygen for insertion into organic substrates.[4] Clearly, a structural and mechanistic understanding of the activation of dioxygen by P-450 will be of considerable use in the design of comparable nonenzymatic catalysts.

$$RH + O_2 + 2e^- + 2H^+ \xrightarrow{\text{cytochrome P-450}} ROH + H_2O \quad (1)$$

Chloroperoxidase is an enzyme isolated from the fungus *Caldarcomyces fumago*.[7] In addition to classical peroxidase and catalase activities exhibited by other peroxidases,[8] chloroperoxidase catalyzes the formation of carbon–halogen bonds between $I^-$, $Br^-$, $Cl^-$, and halogen acceptors such as β-keto

0002-7863/78/1500-7282$01.00/0 

Scheme I

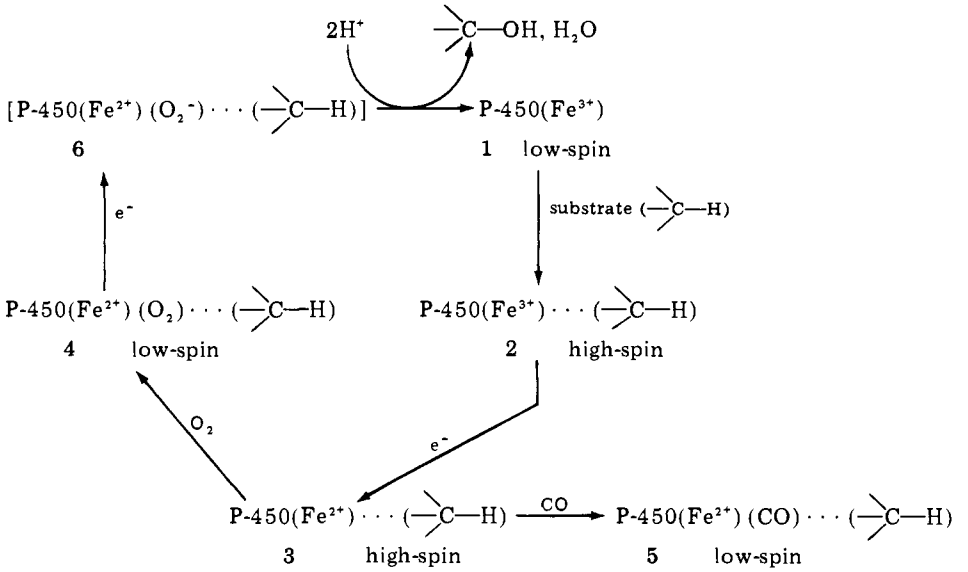


acids, AH (reaction 2). This two-electron oxidative process occurs with concomitant reduction of hydrogen peroxide to water. Chloroperoxidase, as well as horseradish peroxidase, can catalyze chlorination reactions in the absence of chloride and hydrogen peroxide by using chlorite as the source of the incorporated chlorine.[9] In contrast, myeloperoxidase catalyzes chloride-dependent chlorination but is inactivated by chlorite.[10] Information concerning the structure of the active site of chloroperoxidase may help explain the differences between these peroxidases.

$$AH + X^- + H^+ + H_2O_2 \xrightarrow{\text{chloroperoxidase}} AX + 2H_2O \quad (2)$$

The cytochrome P-450 enzymes have a common reaction cycle with four well-characterized states[2] (Scheme I, **1–4**) beginning with a low-spin, six-coordinate ferric resting form, **1,** which is converted upon substrate binding to a high-spin, five-coordinate ferric state, **2.** Reduction gives a high-spin, five-coordinate ferrous complex, **3,** capable of binding dioxygen, **4,** or carbon monoxide, **5.** Addition of a second electron to state **4** leads to formation of the hydroxylated product, presumably after transient formation of a species such as **6.** A question of fundamental importance to the structure and catalytic activity of P-450 is the identity of the nonporphyrin, axial ligand(s) to the central iron in these six states. Substantial progress has been made toward this goal through a comparison of the physical properties of synthetic porphyrin complexes having various axial ligands and myoglobin complexes of known axial histidine ligation with P-450 states **1–5.**[11-13] In this manner, strong evidence has been obtained, principally from EPR, optical absorption, and MCD spectral studies, for the presence of cysteinate sulfur as the axial ligand in states **1, 2,** and **5.** Ferrous thiolate porphyrin complexes have been prepared with properties similar to those of state **3,** strongly suggesting that thiolate ligation is retained upon reduction.[12] Recent spectral studies on oxy-P-450 (**4**) and oxymyoglobin have at least eliminated neutral histidine as a ligand for that state.[13] More detailed knowledge about ligand-iron bond distances should provide insight into the bond strengths in these various states. Such information would certainly be useful in drawing mechanistic conclusions about the activation of dioxygen by P-450.

In contrast to P-450, the catalytic reaction cycle of chloroperoxidase does not involve reduction to the ferrous oxidation level.[14] Instead, initial interaction with hydrogen peroxide leads to an iron oxide species called compound I which is formally two oxidation equivalents above the ferric resting state. Addition of chloride ion and substrate then leads to the chlorinated product and the resting ferric enzyme. Chloroperoxidase is isolated in a predominantly high-spin, ferric form with properties similar to P-450 state **2.**[15] On raising the pH to greater than 7.0, a low-spin ferric form analogous to P-450 state **1** results.[16] Chloroperoxidase can also be reduced to a high-spin ferrous state such as **3** and complexed with carbon monoxide (**5**).[16] The ferrous enzyme is very oxygen sensitive; a stable oxygen complex analogous to state **4** has not been isolated.

Chloroperoxidase strongly resembles P-450 in many of its spectral properties,[15-19] suggesting an underlying structural correspondence between the two enzymes. The most striking similarity is the location of the Soret band of reduced + CO chloroperoxidase at 443 nm and of P-450 at 450 nm as opposed to the 410–420-nm peak found for most other heme-CO complexes.[16] Additional similarities are observed between chloroperoxidase and P-450 in this and other states by optical absorption,[16] MCD,[17] Raman,[18] and Mössbauer[15,19] spectroscopy. This extensive body of spectral data, therefore, also strongly supports cysteinate sulfur ligation for chloroperoxidase. Particularly compelling are the arguments for cysteinate ligation based on a comparison of the MCD spectra of P-450 and chloroperoxidase states **2** and **5** with those of porphyrin model complexes.[17] Only model complexes with thiolate sulfur ligation are able to reproduce the corresponding protein spectra. Despite these spectral lines of evidence in support of cysteinate binding, attempts by Chiang et al.[20] to detect a free sulfhydryl group available for ligation of iron have been unsuccessful. Further spectroscopic and chemical experimentation appears necessary in order to resolve this dilemma.

X-ray absorption spectroscopy has recently proven to be a valuable tool for the study of metalloproteins. Analysis of the extended X-ray absorption fine structure (EXAFS), can atoms surrounding the X-ray absorbing species.[21] Metalloprotein EXAFS data have already been analyzed in order to further characterize the Fe environments in hemoglobin[22] and rubredoxin,[23] the Cu environments in hemocyanin[24] and azurin,[25] as well as the Mo site in nitrogenase.[26]

We present here our initial studies of the ferric resting states of P-450 and chloroperoxidase by X-ray absorption spectroscopy. As an example of the low-spin six-coordinate ferric state, phenobarbital-induced liver microsomal P-450 (PB-P-450-LM2) without added substrate has been examined (Figure 1, **8**), while chloroperoxidase has been studied at room temperature as an example of the high-spin, five-coordinate ferric state (Figure 1, **7**). This particular choice of proteins and conditions was motivated by a desire to avoid samples of mixed

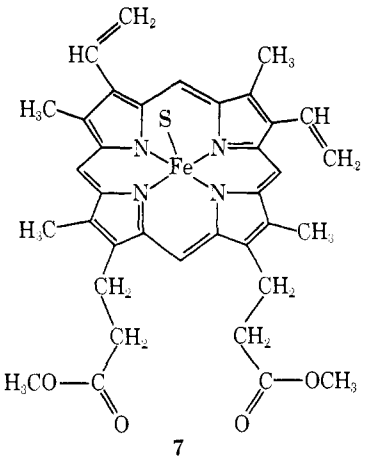

7

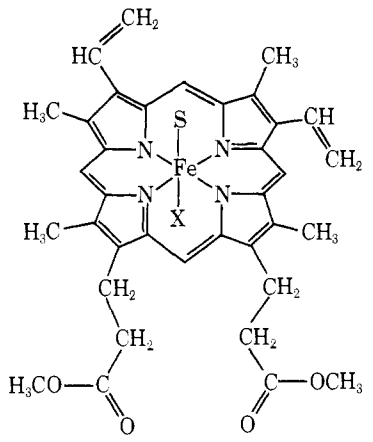

8

**Figure 1.** Structures of high-spin (**7**) and low-spin (**8**) iron protoporphyrin IX dimethyl ester (PPIXDME) complexes.

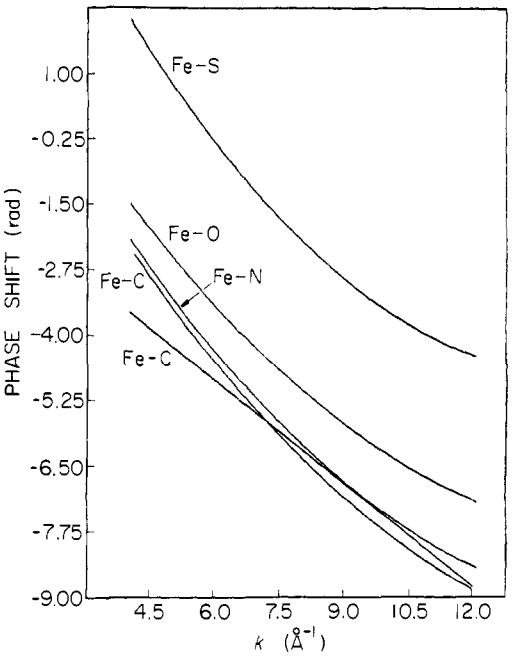


**Figure 2.** Pairwise Fe-X phase shifts used in EXAFS fits. The values were determined using the procedures described in ref 21 and the models listed in the Experimental Section. Two carbon phase shift curves are shown. The upper curve is used to fit first coordination shell carbon distances while the lower Fe-C curve was found to be a better model for α carbons in porphyrin rings.

spin state composition. For example, even when saturated with substrate, PB-P-450-LM2 is only a 1:1 mixture of high- and low-spin species at room temperature, while it is virtually 100% low spin in the absence of substrate.[27] Similarly, at −180 °C chloroperoxidase is a mixture of high- and low-spin forms,[15] whereas at room temperature it is well over 90% high spin.[28] Thus, the data presented here are from the limiting cases of nearly pure high- and low-spin species for these proteins. In addition to verifying the proposed presence of sulfur ligands in both protein states examined, presumably arising from cysteinate ligation, the determination of iron–nitrogen and iron–sulfur bond lengths presented here should provide valuable information upon which to base mechanistic interpretations. In this regard, extension of these studies to the other isolable states of P-450 and chloroperoxidase should be particularly interesting.

## Experimental Section

**Samples.** The compounds $(Et_4N)[Fe(S_2\text{-}o\text{-}xyl)_2]$, $(Et_4N)_2[Fe(S_2\text{-}o\text{-}xyl)_2]$, and $(Et_4N)_2[Fe_4S_4(SCH_2Ph)_4]$ were kindly provided by Dr. Richard H. Holm. These materials were loaded into cells in an inert atmosphere box under dinitrogen. The sample cells were then placed in a small Lucite sample box with Kapton windows, which was sealed under the dinitrogen atmosphere. Finally, this Lucite box was transported to the Stanford Synchrotron Radiation Laboratory (SSRL) in a large sealed glass desiccator vessel containing $N_2$ from which it was removed just prior to the X-ray absorption measurements.

The "picket-fence" porphyrin compounds, Fe(TpivPP)(N-MeIm) and Fe(TpivPP)(N-MeIm)($O_2$), were synthesized and generously donated by Dr. Thomas Halbert in Professor James P. Collman's laboratory. The remaining model compounds were prepared by Dr. Thomas Sorrell, also in Professor Collman's laboratory, according to literature procedures.[11]

Chloroperoxidase was isolated as described previously.[7] It was stored as a concentrated solution (8.7 mg/mL) at 4 °C. Five milliliters of this solution was treated with 3.2 g of $(NH_4)_2SO_4$, and the resultant precipitate was centrifuged to give a hard pellet. The sample had a spectral purity index ($A_{Soret}/A_{280}$) of 1.39 which was essentially unchanged after the actual data collection.

The PB-P-450-LM2 sample was prepared using literature procedures.[27,28] The spectra were recorded on a centrifuged pellet of glycerol precipitated material. Examination of the reduced + CO UV–visible absorption spectrum revealed only negligible contamination by cytochrome P-420, both before and after the sample was exposed to X-rays. The ratio of nmol heme/mg protein was 18.

**Data Collection.** All of the X-ray absorption spectra were recorded using monochromatized radiation at SSRL. The model compound spectra were all recorded in the absorption mode and the energy scales of all spectra were calibrated using an Fe foil, with the first inflection point of the foil spectrum defined as 7111.2 eV.

The chloroperoxidase data were recorded on a sample near room temperature as a fluorescence excitation spectrum, on SSRL line 2 using a Si[1,1,1] channel cut crystal monochromator. The sample was placed in the beam at a 45° angle, and the X-ray intensity perpendicular to the beam was measured. At 3.5 GeV and 27.5 mA, the count rate from the NaI scintillation detector was about $1.5 \times 10^5$ Hz, and about 17% of these counts were due to Fe Kα fluorescence. The spectrum presented represents the average of 16 20-min scans.

The cytochrome P-450 LM2 data were collected on three different occasions and averaged. The data presented represent an average of eight 20-min absorption mode scans on SSRL line 2 with a Si[1,1,1] crystal monochromator, six fluorescence mode scans on line 1 with a Si[2,2,0] crystal, and 15 scans on the focused beam line with a Ge[1,1,1] crystal.

From any given monochromator crystal, the spectra contain instrumental artifacts, "glitches", arising from sudden changes in the monochromated beam intensity and harmonic composition. Some of these fluctuations arise when the crystal orientation allows diversion of part of the Bragg-reflected beam into another reflection, causing a decrease in the primary beam intensity. Because the detectors which measure $I$ and $I_0$ are not perfectly linear, these dips in $I_0$ survive the ratioing process as glitches in the absorption or fluorescence excitation

spectrum. Averaging data from three different crystals after removal of the major glitches significantly improved the quality of the P-450 data and this is the primary reason that the P-450 data are useful over a wider range than the chloroperoxidase data.

**Determination of Empirical Fe-X Phase Shift and Amplitude Functions.** The general philosophy behind structure determination from EXAFS has been outlined previously.[21] Briefly, EXAFS is defined by

$$\chi(k) \equiv \frac{\mu - \mu_S}{\mu_0} \approx \frac{1}{k} \sum_s N_s \frac{|f_s(\pi,k)|}{R_{as}^2} \sin(2R_{as}k + \alpha_{as}(k)) e^{-2\sigma_{as}^2 k^2} \quad (3)$$

where the symbols are identical with those in ref 21. Throughout this work, the approach has been to empirically determine the relevant functions of eq 3 through analysis of the spectra of model compounds of known structure. Once the relevant phase shift and amplitude functions are known, the spectra of unknown compounds can be interpreted to yield structural information. For this particular study, the set of iron model compounds used for determination of the appropriate Fe-X parameters included ferrocene, (Fe-C); [Fe(TPP)-(im)$_2$]Cl, (Fe-N); Fe(acac)$_3$, (Fe-O); [Fe(S$_2$-*o*-xyl)$_2$]$^-$, (Fe-S); and [Fe$_4$S$_4$(SCH$_2$-Ph)$_4$]$^{2-}$, (Fe-Fe). Furthermore, for carbon atoms in the second coordination sphere, a different set of Fe-C parameters was found necessary. The latter values were obtained through analysis of the Fe-C components of Fe(acac)$_3$ and FeTPP EXAFS. The pairwise phase shifts used in the fitting analysis are graphed in Figure 2. In all of the fits, the $E_0$ value used for defining $k = 0$ was 7130 eV.

## Analysis of Iron Porphyrin EXAFS

To establish a basis for interpretation of the protein EXAFS, a set of iron porphyrins with crystallographically known structures was analyzed first. In general, metalloporphyrins have quite complex EXAFS. This is because of the highly symmetric arrangement of porphyrin ring atoms out to more than 4 Å from the central metal atom which contribute many strong high-frequency components to the data. This contrasts with complexes of lower symmetry where the many weak individual contributions from scatterers beyond the first coordination sphere add incoherently and tend to cancel. Thus, porphyrin EXAFS is quite different from the spectra of simpler inorganic complexes (see ref 21 for some examples), in which case contributions from atoms beyond the first coordination sphere can often be neglected.

**Fourier Transforms.** Because of its high symmetry and lack of axial ligands, $\alpha,\beta,\gamma,\delta$-tetraphenylporphinatoiron(II) (FeTPP) serves as a useful benchmark for the understanding of iron porphyrin EXAFS. The EXAFS of this molecule is complex, whether examined directly in $k$ space or as a Fourier transform. Both forms of the data are presented in Figure 3. The Fourier transform of the EXAFS data, taken over a wide $k$ range at liquid nitrogen temperature, reveals seven distinct components which can be accounted for by reference to the structure of FeTPP (indicated by arrows in Figure 3).

The two strongest components of the FeTPP EXAFS arise from the four Fe-N$_P$ and the eight Fe-C$_\alpha$ interactions, and the transform reveals that the former component is about twice as strong as the latter. Because of their longer distance, smaller number, and greater thermal motion, the four Fe-C$_\gamma$ interactions contribute only a minor component to the EXAFS, which is often not resolved from the Fe-C$_\alpha$ peak. The next component, due to eight Fe-C$_\beta$ interactions, is about half the strength of the Fe-C$_\alpha$ contribution.

For tetraphenylporphyrins at low temperatures, one can actually observe higher frequency components in the EXAFS due to the substituent phenyl rings. The first such feature, which is caused by the four phenyl carbons bound to the porphyrin methine bridge, occurs just beyond the Fe-C$_\beta$ peak. One should note that the phase of the first phenyl carbon component is reversed from that of the other peaks in the transform. This is a shadowing effect, arising from the fact that

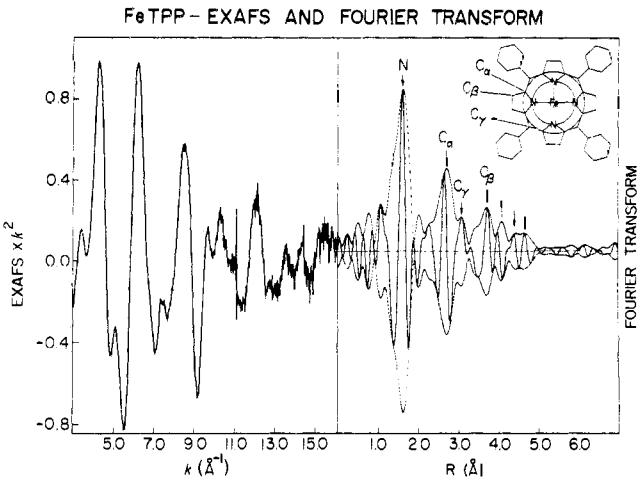


**Figure 3.** EXAFS data (left) and Fourier transform of the data (right) for Fe(TPP). The transform was over a range of $k$ = 4-16 Å$^{-1}$ with $k^3$ scaling. The magnitude is shown superimposed on the imaginary phase component. Note the contribution of neighboring shells even beyond the $\beta$ carbons of the pyrrole rings.

the methine carbons are directly on the line of sight path between the four phenyl carbons and the central iron atom. Just beyond this feature is a final pair of barely resolved peaks, corresponding to the next two shells of eight carbons apiece from the phenyl rings. Thus, under the ideal conditions of high symmetry, low temperature, and good signal to noise, porphyrin EXAFS is actually influenced by atoms as far as 5 Å from the central metal atom.

With less symmetric porphyrins, such as Fe$^{III}$(PPIXDME) with SC$_6$H$_4$-*p*-NO$_2$ or OC$_6$H$_4$-*p*-NO$_2$ axial ligands, the EXAFS becomes even more complicated, and a simple interpretation of the Fourier transform becomes less reliable. The EXAFS transforms for the latter two compounds are compared with that of FeTPP in Figure 4. Apart from the Fe-N$_P$, Fe-C$_\alpha$, and Fe-C$_\beta$ peaks, extra features assignable to Fe-S or Fe-O interactions are observed. Furthermore, the three peaks assigned to Fe-phenyl distances in FeTPP have been replaced by a new group of features from the PPIXDME side chains.

Although the Fourier transforms reveal the general features of the Fe environment, determination of molecular structure from transform peak heights and positions is prone to many artifacts. For example, the primary Fe-N$_P$ peak generally has a low R shoulder which could easily be mistaken for a short axial ligand distance. Similarly, the overlap of Fe-N$_P$ and Fe-C$_\alpha$ side lobes produces a peak between the two major peaks which could again be misinterpreted as an axial ligand distance.

Another important consideration is the fact that on the narrow range of data typically available for hemoprotein EXAFS, many of the transform features discussed above are completely unresolved. For example, using a transform from $k$ = 4-10 Å$^{-1}$, Fe-N$_P$ and Fe-axial ligand contributions combine to form a single broad peak which is useless for distance determinations. The preceding Fourier transforms were certainly useful in a pedagogical sense. However, for the purpose of interpreting the cytochrome P-450 and chloroperoxidase data, it was necessary to develop a procedure which could determine Fe-N$_P$ and Fe-axial ligand distances on a small range of data in $k$ space.

**Curve-Fitting Analysis of Fe Porphyrin EXAFS.** A complete curve-fitting analysis of all the components of an Fe porphyrin EXAFS spectrum would involve too many variables to give reliable structural results;[21] however, the structural features that were of most interest were (1) the type of axial ligand(s),

**Table I.** Iron Porphyrin Curve-Fitting Results[a,d]

| compd | Fe-N | | | Fe-$C_\alpha$ | | | Fe-X | | | |
|---|---|---|---|---|---|---|---|---|---|---|
| | $R_{xtal}$, Å | $R_{EXAFS}$, Å | EXAFS number | $R_{xtal}$, Å | $R_{EXAFS}$, Å | EXAFS number | $R_{xtal}$, Å | $R_{EXAFS}$, Å | EXAFS number | ref |
| Fe(TPP) | 1.972 (4) | 1.979 (2) | 4.4 (1) | $3.016_{av}$ | 3.044 (3) | 7.7 (4) | | | | 43 |
| Fe(TpivPP)-(N-MeIm) | $2.079_{av}$ | 2.073 (2) | 4.1 (2) | $3.089_{av}$ | 3.109 (4) | 7.9 (5) | | | | 44[c] |
| Fe(TpivPP)-(N-MeIm)$O_2$ | $1.998_{av}$ | 2.005 (4) | 4.9 (2) | $3.04_{av}$ | 3.060 (3) | 8.7 (5) | 1.75 (2) | 1.785 (14) | 0.9 (1) | 45 |
| | $1.998_{av}$ | 2.00* | 5* | $3.04_{av}$ | 3.059 (3) | 8.6 (5) | 1.75 (2) | 1.768 (7) | 0.9 (1) | |
| Fe(PPIXDME)-($SC_6H_4$-*p*-$NO_2$) | 2.064 (18) | 2.057 (3) | 4.2 (2) | $3.089_{av}$ | 3.095 (3) | 8.3 (4) | 2.324 (2) | 2.325 (4) | 1.2 (1) | 46 |
| | 2.064 (18) | 2.065* | 4* | $3.089_{av}$ | 3.096 (3) | 8.4 (3) | 2.324 (2) | 2.326 (4) | 1.1 (1) | |
| FeTPP($SC_6H_5$)-($SHC_6H_5$)$_x$ | | 2.037 (3) | 3.5 (2) | | 3.092 (3) | 7.0 (4) | 2.32 (hs) | 2.283 (5) | 1.0 (1) | 32 |
| | | 2.065* | 4* | | 3.096 (3) | 7.0 (4) | | 2.294 (10) | 0.5 (1) | |
| | | 2.040 (3) | 4* | | 3.092 (3) | 7.2 (4) | | 2.294 (4) | 1.0 (1) | |
| Fe(PPIXDME)-($OC_6H_4$-*p*-$NO_2$) | 2.073 (6) | 2.055 (3) | 4.5 (2) | $3.102_{av}$ | 3.086 (3) | 8.0 (4) | 1.842 (4) | 1.839 (7) | 1.6 (1) | 47[b] |
| | 2.073 (6) | 2.065* | 4* | $3.102_{av}$ | 3.087 (3) | 8.0 (4) | 1.842 (4) | 1.862 (4) | 1.7 (1) | |
| $(FeTPP)_2O$ | 2.087 (3) | 2.079 (2) | 3.8 (2) | $3.102_{av}$ | 3.096 (5) | 5.5 (5) | 1.763 (1) | 1.754 (8) | 0.9 (1) | 48 |
| | 2.087 (3) | 2.065* | 4* | $3.102_{av}$ | 3.093 (5) | 5.5 (5) | 1.763 (1) | 1.748 (6) | 1.2 (1) | |

[a] Numbers with asterisks were fixed at these values during fit. [b] Distances quoted are for Fe(PPIXDME)($OCH_3$). [c] Distances quoted are for Fe(TpivPP)(2-MeIm). [d] The values in parentheses after the EXAFS numbers are the calculated fitting errors. From comparison with the crystallographic data, it is clear that the systematic errors in the curve-fitting calculations are substantially larger than the statistical fitting errors.

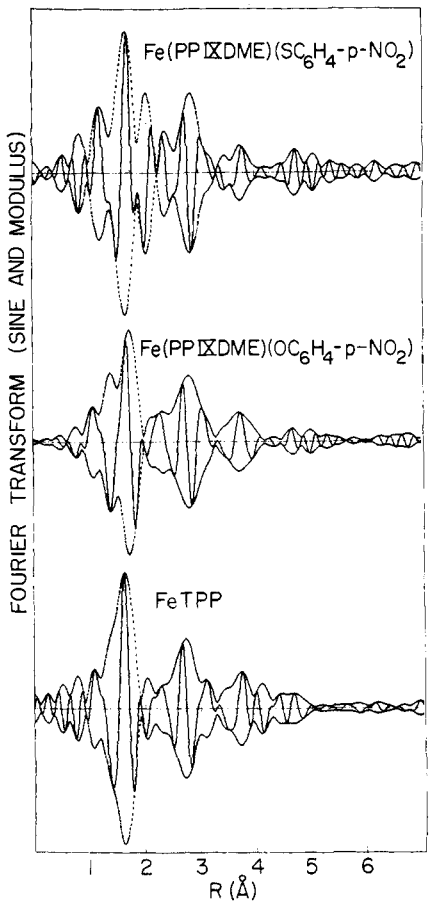


**Figure 4.** Fourier transforms of porphyrins with a sulfur axial ligand (top), an oxygen axial ligand (middle), and no axial ligands (bottom). The transforms were over the range of $k$ = 4–16 Å$^{-1}$ with $k^3$ weighting. The modulus of each transform is shown superimposed on the sine component.

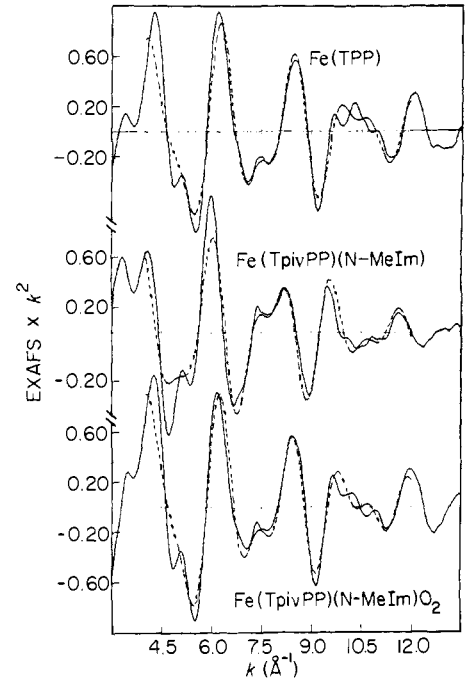


**Figure 5.** Least-squares fits (dashed lines) to EXAFS data (solid lines) for structure determination. The upper two fits include only N and $C_\alpha$ waves (four variables in each fit). The lower fit included a third wave for the oxygen atom (giving six variables in the fit). All fits were over a range of $k$ = 4–12 Å$^{-1}$ and the numerical results of the fits are summarized in Table I.

X, and the Fe-X distance(s); (2) the Fe-$N_P$ distance; and (3) the geometry of the Fe with respect to the mean porphyrin plane. For the present analysis, the curve-fitting procedure has simply used a three-wave fit involving (1) an Fe-X wave, (2) an Fe-$N_P$ wave, and (3) an Fe-$C_\alpha$ wave.

Although Fourier filtering to remove frequency components higher than those from Fe-$C_\alpha$ did improve the quality of the fits, it did not significantly improve the accuracy of the numbers obtained. This is because the components beyond Fe-$C_\alpha$ are of sufficiently high frequency and small magnitude as to be relatively uncorrelated with the shorter distance contributions.

Because it is devoid of axial ligands, the simplest porphyrin for curve-fitting analysis was FeTPP. Only two waves were used to fit the EXAFS in this case, one for the Fe-N component and one for the Fe-$C_\alpha$ component. The resulting fit (Figure 5) predicted an Fe-N distance within 0.007 Å of the crystallographic value,[30] while the Fe-$C_\alpha$ distance was within 0.028 Å. The quality of the fit using four variables was extremely gratifying, considering the number of components

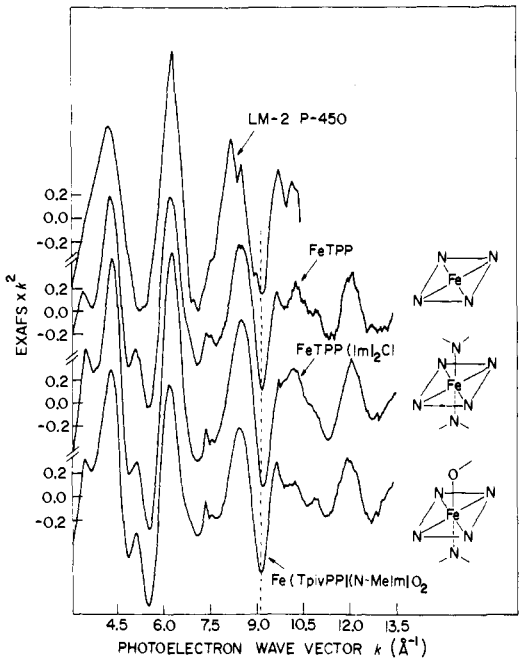


**Figure 6.** Comparison of LM-2-P-450 EXAFS data with other low-spin Fe porphyrins. The dotted line is shown to facilitate visual comparison of the dip in the EXAFS data at $k \approx 9$ Å$^{-1}$. For low-spin (Fe in plane) porphyrins this dip is somewhat above 9 Å$^{-1}$, while for high-spin porphyrins (see Figure 7) the dip occurs below 9 Å$^{-1}$. The effects are discussed in detail in the text.

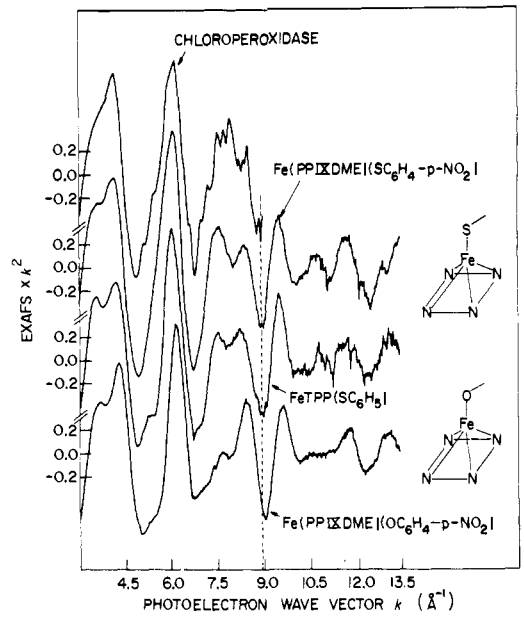


**Figure 7.** Comparison of chloroperoxidase EXAFS data with that of two high-spin (Fe out of plane) porphyrins. As in Figure 6, the dotted line indicates the position of the maximum in the data around $k \approx 9$ Å$^{-1}$. Note the distinct similarity between the chloroperoxidase and the Fe(PPIXDME)($SC_6H_5$-*p*-$NO_2$) EXAFS data.

being neglected, and the fact that a worse fit was obtained 2 years ago with 12 variables.[31]

A similar two-wave fit was done on the EXAFS data for Fe(TpivPP)(N-MeIm) (Figure 5). Since an extra wave for the axial Fe-$N_{im}$ component was not included, the Fe-N distance of 2.073 Å obtained from this fit is a weighted average of Fe-$N_P$ and Fe-$N_{im}$ distances. If one assumed that the Fe-$N_{im}$ distance in the unhindered (N-MeIm) compound was the same as the 2.108 Å value reported for the sterically hindered (2-MeIm) compound,[32] then the average Fe-$N_P$ distance would be calculated to be 2.064 Å. Since the axial imidazole Fe-N distance is probably shorter in the present case, 2.064 Å is probably a low estimate of the Fe-$N_P$ distance.

This value is slightly different from the value of 2.055 Å obtained by Shulman et al. for the same compound.[22a] Further discussion of this small difference will not be fruitful until a reliable crystal structure for Fe(TpivPP)(N-MeIm) is available. However, it should be noted that the latter group claimed that their shorter bond length for a ferrous porphyrin was significant, compared to a typical ferric porphyrin Fe-$N_P$ distance of 2.065 Å. The current results indicate that the ferrous Fe-$N_P$ bond length is on the order of 2.07 Å.

The three-wave fits required the addition of a third wave to characterize one of the Fe-axial ligand distances. For example, oxygenation of the "picket-fence" compound to yield Fe(TpivPP)(N-MeIm)$O_2$ results in a substantial change in the EXAFS (Figure 5), the bulk of which is due to changing Fe-$N_P$ and Fe-$C_\alpha$ distances. Adding a third wave to the fit yielded a 1.79 (3) Å prediction for the Fe-O distance, slightly longer than the crystallographic value of 1.75 (2) Å. Constraining the Fe-N distance closer to the crystallographic average shortened the calculated Fe-O distance to 1.77 Å, which is the best estimate possible with the current analysis procedure.

Although the calculated scatterer numbers were often quite good, in several of the remaining three-wave fits there were discrepancies which should be discussed. For example, the Fe-$C_\alpha$ number in the $(FeTPP)_2O$ fit is probably low because of destructive interference with an Fe-Fe component at nearly the same frequency. The large value for the oxygen amplitude for Fe(PPIXDME)($OC_6H_4$-*p*-$NO_2$) (1.6) relative to amplitudes in $(FeTPP)_2O$ (0.9) and Fe(TpivPP)(N-MeIm)$O_2$ (0.9) probably reflects the fact that the data for the first compound were collected at liquid nitrogen temperature, while data for the latter two compounds and the Fe(acac)$_3$ model were collected at room temperature, with consequent higher thermal motion.

The compound which gave the most troublesome results was Fe(TPP)($SC_6H_5$)($HSC_6C_5$). The fact that both Fe-N and Fe-S distances are intermediate between the expected high- and low-spin values makes it appear that the room temperature data represent a mixture of spin states. This is in agreement with results obtained by Collman et al. on this compound.[11e] The danger of studying inhomogeneous or impure model compounds or protein samples is clear. EXAFS analysis of such mixtures will simply yield average values for the distances present, with only mild indications, such as reduced amplitudes, that a single structure is not present.

For the 11 distances which are exactly comparable with crystallographically known values. the average deviation of the EXAFS prediction was 0.012 Å. The average deviation was 0.007 Å for Fe-N distances, 0.022 Å for Fe-O distances, 0.015 Å for Fe-$C_\alpha$ distances, and 0.001 Å for the single Fe-S distance in Fe(PPIXDME)($SC_6H_4$-*p*-$NO_2$). The scatterer number calculations were considerably less precise than the distance determinations, yet in most cases with appropriate rounding they gave the correct number of atoms.

## Cytochrome P-450-LM2 and Chloroperoxidase

**General Features.** Under the experimental conditions used for EXAFS data collection, the iron in PB-P-450-LM2 was essentially all in the low-spin ferric state,[27] while the chloroperoxidase iron was almost completely high spin.[28] EXAFS does not directly sense the spin state of the iron, but it is sensitive to the position of the iron with respect to the porphyrin ring. In heme chemistry high-spin compounds are generally five coordinate with out of plane iron,[33] while low-spin compounds have six-coordinate iron approximately in the porphyrin plane. Accordingly, in Figure 6, the P-450-LM2

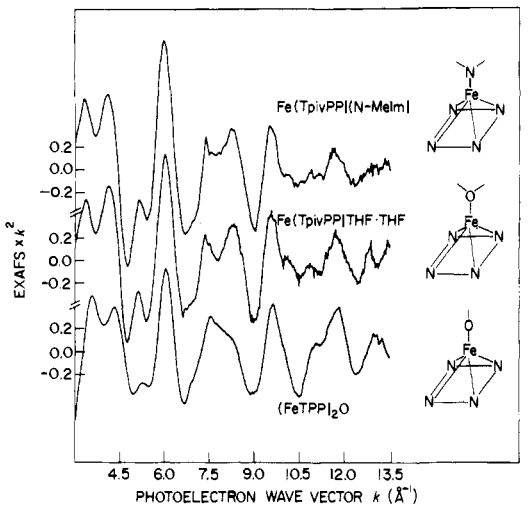


**Figure 8.** Additional EXAFS data for high-spin Fe porphyrins. These data may be compared with those for chloroperoxidase shown in Figure 7.

EXAFS is compared with several porphyrins that have in-plane iron, while in Figure 7 chloroperoxidase is compared with several five-coordinate out of plane Fe porphyrins. Figure 8 presents additional high-spin Fe porphyrins to compare with chloroperoxidase.

The basic features of all iron porphyrin spectra are dominated by the alternating constructive and destructive interference between the Fe-$N_P$ and Fe-$C_\alpha$ components. However, because of the number of other frequency components present in the EXAFS, this beat pattern is not always clear. The strongest beats occur as a sharp peak just beyond $k$ of 6 Å$^{-1}$, where both components are in phase and positive, and near 9 Å$^{-1}$, where in-phase negative contributions cause a strong dip in the EXAFS.

The minimum in the vicinity of 9 Å$^{-1}$ is primarily determined by the Fe-$N_P$ and Fe-$C_\alpha$ components, and it is relatively insensitive to the nature of or distances to the axial ligands. It, therefore, could serve as a useful indicator of the position of the Fe with respect to the porphyrin. For porphyrins with in-plane iron, this dip generally occurs slightly after $k$ = 9 Å$^{-1}$, while, because of the longer Fe-porphyrin distances with out of plane structures, the dip for the latter occurs slightly before 9 Å$^{-1}$. As expected, the P-450-LM2 dip occurs beyond 9 Å$^{-1}$, classifying its Fe as approximately in plane, while the chloroperoxidase dip before 9 Å$^{-1}$ suggests that Fe is out of plane in this protein (see Figures 6 and 7).

Although the dominant beat pattern of Fe porphyrin EXAFS is determined by the Fe-$N_P$ and Fe-$C_\alpha$ components, with significant contributions by Fe-$C_\gamma$ and Fe-$C_\beta$ terms as well, there are also variations in peak splittings and relative peak heights caused by the presence of the axial ligands. With a representative set of model compounds, one can therefore "fingerprint" the possible types of Fe coordination spheres. Provided that one has a sufficiently good set of models, simple matching of model compound and protein spectra is a means of interpreting the EXAFS independent of Fourier transform or curve-fitting analysis. Such comparison methods are useful as a means for obtaining an initial guess at the protein structure, which can subsequently be refined by curve-fitting methods.

From slightly beyond $k$ = 3.2 Å$^{-1}$ to just before 9 Å$^{-1}$ there are three major maxima and two major minima in the EXAFS of all high-spin porphyrins. One can compare the EXAFS of chloroperoxidase with the six models of Figures 7 and 8 on the basis of whether or not corresponding peaks and valleys are split and, if so, whether relative peak heights of split features are similar. Using such criteria, Table II was constructed.

**Table II.** Comparison of Chloroperoxidase EXAFS with Known Structures[a]

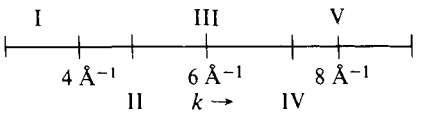


| structure | region I | II | III | IV | V |
|---|---|---|---|---|---|
| Fe(PPIXDME)$SC_6H_5$-$p$-$NO_2$ | + | + | + | + | + |
| Fe(TPp)($SC_6H_5$)($SHC_6H_5$) | + | ? | + | + | ? |
| Fe(PPIXDME)$OC_6H_5$-$p$-$NO_2$ | + | ? | + | − | − |
| $(FeTPP)_2O$ | − | − | + | ? | ? |
| Fe(TpivPP)N-MeIm | − | − | + | ? | − |
| Fe(TpivPP)THF | − | − | + | + | − |

[a] +, good match; ?, ambiguous; −, clear mismatch.

The results of this correspondence table and simple visual inspection of the EXAFS data show that only Fe porphyrins with axial thiolate ligands provide a good match to the chloroperoxidase EXAFS. The best correspondence occurs with Fe(PPIXDME)($SC_6H_4$-$p$-$NO_2$), and inspection of Figure 7 shows that the spectra of chloroperoxidase and the latter compound are nearly superimposable. The optical, EPR, and Mössbauer spectra of Fe(PPIXDME)($SC_6H_4$-$p$-$NO_2$) have previously been shown to mimic those of high-spin P-450,[11a] which in turn are very similar to the chloroperoxidase spectra. The most reasonable conclusion from the EXAFS data is that chloroperoxidase has an axial cysteine thiolate bound to the iron.

For low-spin P-450-LM2, none of the available in-plane Fe porphyrin spectra bears much resemblance to the protein EXAFS. The same pattern of peak splittings and relative intensities is observed in FeTPP, $FeTPP(Im)_2Cl$, and Fe(TpivPP)(N-MeIm)$O_2$. The spectra presented indicate that the EXAFS is fairly insensitive to the presence or absence of axial nitrogen or oxygen ligands, as long as the iron-porphyrin distances remain about the same.

The cytochrome P-450 EXAFS has a radically different appearance from the other in-plane porphyrins. The sharp subsidiary maxima and minima of the other in-plane spectra are gone, and a relatively broad and featureless spectrum is obtained. Such a result is consistent with, although not proof for, the presence of a sulfur ligand. This is because the electron backscattering amplitude of S is more than twice as large in magnitude and almost $\pi$ out of phase with the comparable N function. Thus, the presence of an axial sulfur ligand would contribute a relatively large component substantially out of phase with the Fe-$N_P$ EXAFS, thereby broadening the fairly sharp features of the porphyrin EXAFS.

The visual comparison results may be summarized as follows. A qualitative impression of sulfur ligation for both chloroperoxidase and cytochrome P-450-LM2 can be gained from inspection of the protein EXAFS and comparison with model compound data. In order to make quantitative structural conclusions about the Fe coordination sphere in these two proteins, three-wave curve-fitting studies analogous to those used with the model compounds have been performed.

**Curve-Fitting Analysis.** The cytochrome P-450-LM2 and chloroperoxidase EXAFS were fitted with the sum of an Fe-$N_P$ wave, an Fe-$C_\alpha$ wave, and either an Fe-S wave or an Fe-O wave for the axial ligand. Because of the similarity in Fe-N and Fe-O phase shifts, the latter fits cover cases involving either axial nitrogen or oxygen ligation. The results of these three wave fits are summarized in Table III, and the best fits are shown in Figure 9. In some of the fits, the Fe-N distances and amplitudes were constrained to typical values found in known porphyrin structures, thereby reducing the number

**Table III.** Summary of Cytochrome P-450 and Chloroperoxidase Curve-Fitting Results[a]

| protein | Fe-N $R_{EXAFS}$, Å | Fe-N EXAFS number | Fe-$C_\alpha$ $R_{EXAFS}$, Å | Fe-$C_\alpha$ EXAFS number | postulated type | Fe-X $R_{EXAFS}$, Å | Fe-X EXAFS number | minimization function[b] |
|---|---|---|---|---|---|---|---|---|
| LM-2 P-450 | 2.001 (3) | 4.8 (3) | 3.068 (5) | 5.1 (5) | S | 2.187 (8) | 0.8 (1) | 0.879 |
| LM-2 P-450 | 2.00* | 5* | 3.068 (5) | 5.2 (4) | S | 2.194 (5) | 0.7 (1) | 0.882 |
| LM-2 P-450 | 2.00* | 4* | 3.066 (6) | 4.9 (4) | S | 2.181 (4) | 1.1 (1) | 0.895 |
| LM-2 P-450 | 1.98* | 4* | 3.059 (5) | 5.0 (5) | S | 2.198 (3) | 1.4 (1) | 1.011 |
| LM-2 P-450 | 1.98* | 5* | 3.061 (5) | 5.5 (5) | S | 2.213 (4) | 1.1 (1) | 1.061 |
| LM-2 P-450 | 2.012 (2) | 6.6 (2) | 3.073 (5) | 5.4 (4) | O | 1.775 (2) | 0.5 (1) | 0.937 |
| LM-2 P-450 | 2.00* | 5* | 3.073 (5) | 5.8 (5) | O | 1.971 (5) | 1.1 (1) | 1.011 |
| LM-2 P-450 | 2.00* | 4* | 3.073 (5) | 5.8 (5) | O | 1.955 (5) | 1.8 (1) | 1.028 |
| chloroperoxidase | 2.047 (3) | 4.2 (3) | 3.087 (5) | 5.7 (4) | S | 2.303 (8) | 0.9 (1) | 0.711 |
| chloroperoxidase | 2.065* | 4* | 3.083 (5) | 5.9 (4) | S | 2.269 (6) | 0.7 (1) | 0.744 |
| chloroperoxidase | 2.090 (4) | 6.0 (4) | 3.084 (4) | 22.6 (1.4) | O | 1.863 (13) | 1.3 (2) | 0.713 |

[a] Numbers with asterisks were constrained to these values during fit. Numbers in parentheses are fitting errors, which are significantly smaller than systematic errors. [b] $F = SQRT\ [\Sigma w(\text{data-fit})^2/N]$; $w = k^6$ and $N$ is the number of points.

of variables to four. In other fits all six variables were unconstrained. Regardless of how the fits were done, in all cases the P-450 and chloroperoxidase EXAFS were best fit by including an axial sulfur ligand, and the calculated Fe-S distances indicated that the sulfur most likely was a cysteine thiolate ligand.

The calculated distances in the best chloroperoxidase fit were Fe-$N_P$ = 2.05 ± 0.03 Å, Fe-$C_\alpha$ = 3.09 ± 0.03 Å, and Fe-S = 2.30 ± 0.03 Å. Although another good fit could be obtained using an oxygen axial ligand, this was only at the expense of unreasonable nitrogen and carbon amplitudes. Given the minimal range of data, there exists a significant amount of correlation between parameters and a number of false minima for the fits. Despite these numerical problems, the spectral similarity of chloroperoxidase with Fe(PPIXDME)($SC_6H_4$-*p*-$NO_2$) and the good agreement of the calculated distances with the known structure makes the conclusion of sulfur ligation inescapable.

The best fit for the P-450-LM2 EXAFS gave distances and amplitudes consistent with an in-plane six-coordinate Fe: Fe-$N_P$ = 2.00 ± 0.03 Å, Fe-$C_\alpha$ = 3.07 ± 0.03 Å, Fe-S = 2.19 ± 0.03 Å. None of the fits using an oxygen axial ligand gave results as good as corresponding fits presuming axial sulfur. Furthermore, constraining the Fe-N distance and amplitude to reasonable values substantially worsened the fits when an axial oxygen was assumed. However, when an axial sulfur ligand was assumed, constraining the Fe-N distance and amplitude to standard values did not significantly change the quality of the fits.

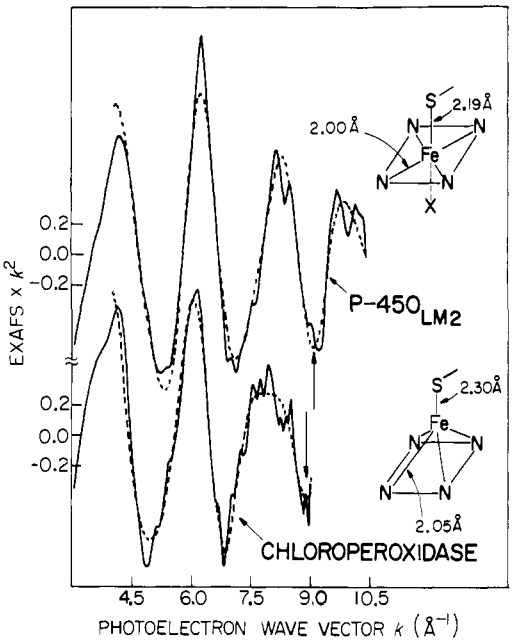


**Figure 9.** Three-wave curve-fitting analysis of LM-2-P-450 and chloroperoxidase data. The least-squares fits (dashed line) to the data (solid line) were carried out over a $k$ range of 4–10.5 $Å^{-1}$ for the P-450 and 4–9.0 for the chloroperoxidase. The numerical results of the fits are summarized in Table III.

## Discussion and Conclusions

The characterization of the Fe environments in P-450-LM-2 and chloroperoxidase proceeded in three distinct stages. The first stage involved the use of the empirical phase shift and amplitude functions to determine interatomic distances in Fe porphyrin models from EXAFS. A curve-fitting procedure was developed which used three waves to characterize the Fe-$N_P$, Fe-$C_\alpha$, and axial Fe-X components of porphyrin EXAFS spectra. Using this method, average Fe-N distances were determined with a mean deviation of 0.007 Å, while Fe-$C_\alpha$ and Fe-X distances were always determined to better than 0.025 Å. Second, visual comparison of the chloroperoxidase and P-450-LM2 EXAFS data with that of model complexes suggested that the iron was high and low spin, respectively, in the two proteins. Visual comparison also suggested the presence of axial sulfur ligation to Fe in both cases. Finally, application of the established curve-fitting procedures confirmed these hypotheses and determined values for the Fe-$N_P$, Fe-$C_\alpha$, and Fe-S distances.

The calculated distances in chloroperoxidase are within 0.02 Å of the known distances in Fe(PPIXDME)($SC_6H_4$-*p*-$NO_2$).[11a] Considering the similarity of the EXAFS between these two samples, calculation of nearly identical distances is hardly surprising. The fact that the distances calculated for chloroperoxidase tended to be slightly shorter than those for the model compound may indicate the presence of a small amount of low-spin material in the protein, rather than a significant structural difference between the model and the protein.

For chloroperoxidase, the conclusion about thiolate ligation is in contradiction with previous chemical work which found that the only two cysteine residues present in the protein were bound in a disulfide bridge.[20] The latter conclusion has already been questioned because of the close spectral similarity between chloroperoxidase and P-450.[17] It would be quite disturbing if all the unique spectral properties of cytochrome P-450, which had been explained by the presence of cysteine thiolate coordination, were reproduced in a protein without such ligation. The EXAFS result points conclusively toward the presence of an iron-sulfur interaction. Despite the lack of

chemical evidence for an available cysteine ligand, the spectroscopic case for sulfur ligation in chloroperoxidase seems complete.

Because of the wealth of spectroscopic information suggesting cysteine thiolate ligation in cytochrome P-450, the EXAFS results predicting a sulfur ligand come as no surprise. *However, EXAFS has been the first technique to yield quantitative information about the Fe–S bond length.* The calculated Fe–S distance of 2.19 ± 0.03 Å in low-spin P-450 is significantly shorter than the 2.30 ± 0.03 Å value obtained for chloroperoxidase. The only available low-spin ferric thiolate porphyrin structure is for $Fe(TPP)(SC_6H_5)(SHC_6H_5)$ at 115 K, for which the Fe–S (thiolate) distance was 2.26 Å. However, in this crystal structure the low-spin iron species is in equilibrium with a high-spin iron structure in approximately a 2:1 ratio.[11e] Perhaps a more representative low-spin ferric thiolate distance is the value of 2.21 Å obtained for the Fe–S distance in $Fe(SC_6H_4CHNCH_2CH_2NH_2)_2$.[34] Substantial shortening of the Fe–S distance upon going from high-spin to low-spin $Fe^{III}$ has also been observed in dithiocarbamate complexes.[35] Thus, the shorter Fe–S distance in low-spin P-450 relative to high-spin chloroperoxidase is in accord with known structural chemistry.

The relatively large amplitude of the Fe–N component makes it tempting to conclude that the sixth ligand in low-spin P-450 is a histidine imidazole nitrogen. In a similar case, the three-wave fit of Fe(TpivPP)(N-MeIm)$O_2$ resulted in a calculated Fe–N amplitude of 4.9 N. However, for Fe(TpivPP)(N-MeIm) only 4.1 rather than 5 N was calculated. Ideally, relative Debye–Waller factors must be considered in these calculations, but for fits on 4–12 $Å^{-1}$ correlation effects preclude inclusion of extra parameters to account for different degrees of thermal motion. Thus, the average error in the Fe–N amplitudes is sufficiently high that the current results indicating imidazole must be considered suggestive rather than conclusive.

The wealth of intermediate states available for P-450-type enzymes makes it clear that this present work is only a preliminary step in the structural characterization of these enzymes. The EXAFS technique has promising applications for characterization of the remaining stages of the catalytic cycle. For example, accurate measurement of the Fe–S bond lengths in the reduced and the oxygenated forms of P-450 should help in deciding whether or not the sulfur ligand becomes protonated in either of these species. Further improvement in both analysis techniques and in data collection procedures still appears possible. The combination should permit analysis of all the Fe–porphyrin distances in these proteins.

**Acknowledgments.** We wish to thank Professors James P. Collman and Richard H. Holm and Drs. Thomas R. Halbert and Thomas N. Sorrell for providing a number of the porphyrin samples used in this analysis. We also thank Professors Seb Doniach, C. Djerassi and J. Trudell and Dr. E. Bunnenberg for their interest in and discussions about this work. K.O.H. is a Fellow of the Alfred P. Sloan Foundation, S.P.C. was an IBM Doctoral Fellow for 1976–1977, and J.H.D. is a recipient of an NIH postdoctoral award from the NCI, F-32-CA0548. This research was supported primarily by the National Science Foundation through Grant PCM-75-17105. Synchrotron radiation time was provided by the Stanford Synchrotron Radiation Laboratory, supported by National Science Foundation Grant DMR-7727498 in cooperation with the Stanford Linear Accelerator Center and the Department of Energy.

## References and Notes

(1) (a) Stanford University; (b) California Institute of Technology; (c) University of Illinois.
(2) I. C. Gunsalus, T. C. Pederson, and S. G. Sligar, *Annu. Rev. Biochem.*, **44**, 377 (1975).
(3) D. F. Brook and P. J. Large, *Eur. J. Biochem.*, **55**, 601 (1975).
(4) Under the proper conditions, however, chloroperoxidase[5] and hemoglobin[6] will catalyze hydroxylation reactions.
(5) P. F. Hollenberg and L. P. Hager, IUB Symposium on Reaction Mechanisms of P-450 and Related Enzymes, Stockholm, 1973.
(6) J. J. Mieyal, R. S. Ackerman, J. L. Blumer, and L. S. Freeman, *J. Biol. Chem.*, **241**, 1763 (1966).
(7) D. R. Morris and L. P. Hager, *J. Biol. Chem.*, **241**, 1763 (1966).
(8) B. C. Saunders, "Inorganic Biochemistry", Vol. 2, G. I. Eichhorn, Ed., Elsevier, Amsterdam, 1973, Chapter 28.
(9) P. F. Hollenberg, T. Rand-Meir, and L. P. Hager, *J. Biol. Chem.*, **249**, 5816 (1974).
(10) J. E. Harrison and J. Schultz, *J. Biol. Chem.*, **251**, 1371 (1976).
(11) (a) S. Koch, S. C. Tang, R. H. Holm, R. B. Frankel, and J. A. Ibers, *J. Am. Chem. Soc.*, **97**, 916 (1975); (b) R. H. Holm, S. C. Tang, S. Koch, G. C. Papaefthymiou, S. Foner, R. B. Frankel, and J. A. Ibers, *Adv. Exp. Med. Biol.*, **74**, 321 (1976); (c) S. C. Tang, S. Koch, G. C. Papaefthymiou, S. Foner, R. B. Frankel, J. A. Ibers, and R. H. Holm, *J. Am. Chem. Soc.*, **98**, 2414 (1976); (d) J. P. Collman, T. N. Sorrell, and B. M. Hoffman, *ibid.*, **97**, 913 (1975); (e) J. P. Collman, T. N. Sorrell, K. O. Hodgson, A. K. Kulshresta, and C. E. Strouse, *ibid.*, **99**, 5180 (1977); (f) H. Ogoshi, H. Sugimoto, and Z. Yoshida, *Tetrahedron Lett.*, 2289 (1975); (g) J. H. Dawson, R. H. Holm, J. R. Trudell, G. Barth, R. E. Linder, E. Bunnenberg, C. Djerassi, and S. C. Tang, *J. Am. Chem. Soc.*, **98**, 3707 (1976); (h) J. O. Stern and J. Peisach, *J. Biol. Chem.*, **249**, 7495 (1974); (i) J. P. Collman and T. N. Sorrell, *J. Am. Chem. Soc.*, **97**, 4133 (1975); (j) J. P. Collman, T. N. Sorrell, J. H. Dawson, J. R. Trudell, E. Bunnenberg, and C. Djerassi, *Proc. Natl. Acad. Sci. U.S.A.*, **73**, 6 (1976); (k) J. P. Collman and T. N. Sorrell, *ACS Symp. Ser.*, **44**, 27 (1977).
(12) (a) C. K. Chang and D. Dolphin, *J. Am. Chem. Soc.*, **97**, 5948 (1975); (b) C. K. Chang and D. Dolphin, *Proc. Natl. Acad. Sci. U.S.A.*, **73**, 3338 (1976); (c) J. P. Collman, T. N. Sorrell, and J. H. Dawson, unpublished results.
(13) J. H. Dawson and S. P. Cramer, *FEBS Lett.*, **88**, 127 (1978).
(14) L. P. Hager, P. F. Holldenberg, T. Rand-Meir, R. Chiang, and D. Doubek, *Ann. N.Y. Acad. Sci.*, **244**, 80 (1975).
(15) P. M. Champion, E. Münck, P. G. Debrunner, P. F. Hollenberg, and L. P. Hager, *Biochemistry*, **12**, 426 (1973).
(16) P. F. Hollenberg and L. P. Hager, *J. Biol. Chem.*, **248**, 2630 (1973).
(17) J. H. Dawson, J. R. Trudell, G. Barth, R. E. Linder, E. Bunnenberg, C. Djerassi, R. Chiang, and L. P. Hager, *J. Am. Chem. Soc.*, **98**, 3709 (1976).
(18) P. M. Champion, R. D. Remba, R. Chiang, D. B. Fitchen, and L. P. Hager, *Biochim. Biophys. Acta*, **446**, 486 (1976).
(19) P. M. Champion, R. Chiang, E. Münck, P. Debrunner, and L. P. Hager, *Biochemistry*, **14**, 4159 (1975).
(20) R. Chiang, R. Makino, W. E. Spooner, and L. P. Hager, *Biochemistry*, **14**, 4166 (1975).
(21) S. P. Cramer, K. O. Hodgson, E. I. Stiefel, and W. E. Newton, *J. Am. Chem. Soc.*, **100**, 2748 (1978).
(22) (a) P. N. Eisenberger, R. G. Shulman, B. M. Kincaid, G. S. Brown, and S. Ogawa, *Nature (London)*, **274**, 30 (1978); (b) P. N. Eisenberger, R. G. Shulman, G. S. Brown, and S. Ogawa, *Proc. Natl. Acad. Sci. U.S.A.*, **73**, 491 (1976).
(23) (a) D. E. Sayers, E. A. Stern, and J. R. Herriot, *J. Chem. Phys.*, **64**, 427 (1976); (b) B. Bunker and E. A. Stern, *Biophys. J.*, **19**, 253 (1977); (c) R. G. Shulman, P. Eisenberger, W. E. Blumberg, and N. A. Stombaugh, *Proc. Natl. Acad. Sci. U.S.A.*, **72**, 4003 (1975); (d) R. G. Shulman, P. Eisenberger, B. K. Teo, B. M. Kincaid, and G. S. Brown, *J. Mol. Biol.*, in press.
(24) T. K. Eccles, Ph.D. Thesis, Stanford University, 1977.
(25) T. D. Tullius, P. Frank, and K. O. Hodgson, *Proc. Natl. Acad. Sci. U.S.A.*, in press.
(26) (a) S. P. Cramer, K. O. Hodgson, W. O. Gillum, and L. E. Mortenson, *J. Am. Chem. Soc.*, **100**, 3398 (1978); (b) S. P. Cramer, W. O. Gillum, K. O. Hodgson, L. E. Mortenson, E. I. Stiefel, J. R. Chisnell, W. J. Brill, and V. K. Shah, *ibid.*, **100**, 3814 (1978).
(27) J. H. Dawson, J. R. Trudell, R. E. Linder, G. Barth, E. Bunnenberg, and C. Djerassi, *Biochemistry*, in press.
(28) J. H. Dawson, Ph.D. Thesis, Stanford University, Stanford, Calif., 1976.
(29) S. P. Cramer, Ph.D. Thesis, Stanford University, Stanford, Calif., 1977.
(30) J. P. Collman, J. L. Hoard, N. Kim, G. Lang, and C. R. Reed, *J. Am. Chem. Soc.*, **97**, 2676 (1975).
(31) S. P. Cramer, T. K. Eccles, F. Kutzler, K. O. Hodgson, and S. Doniach, *J. Am. Chem. Soc.*, **98**, 8059 (1976).
(32) J. P. Collman, private communication of results to be published.
(33) (a) J. F. Deatherage, R. S. Lee, and K. Moffatt, *J. Mol. Biol.*, **104**, 723 (1976); (b) R. C. Lander, E. J. Heidner, and M. F. Perutz, *Ibid.*, in press.
(34) G. D. Fallon and B. M. Gatehouse, *J. Chem. Soc., Dalton Trans.*, 1344 (1975).
(35) E. J. Cukauskas, B. S. Deaver, Jr., and E. Sinn, *J. Chem. Phys.*, **67**, 1257 (1977).